SAND2017-2146C

10th U.S. National Combustion Meeting
Organized by the Eastern States Section of the Combustion Institute
April 23–26, 2017
College Park, Maryland

Numerical study of pyrolysis and combustion of a carbon fiber-epoxy composite

*Heeseok Koo[1,**], Alexander L. Brown[1], Tyler Voskuilen[2], and Flint Pierce[2]*

[1]*Fire Science and Technology, Sandia National Laboratories, PO Box 5800, MS 1135, Albuquerque, NM 87185-1135, USA* [*]
[2]*Compuational Thermodynamics and Fluid Mechanics, Sandia National Laboratories, PO Box 5800, MS 0828, Albuquerque, NM 87185-0828, USA*
[**]*Corresponding author:* `hkoo@sandia.gov`

Abstract: With growing use of carbon fiber-epoxy in transportation systems, it is important to understand fire reaction properties of the composite to ensure passenger safety. Recently, a micro-scale pyrolysis study and macro-scale fire tests were performed using carbon fiber-epoxy at Sandia National Laboratories. Current work focuses on numerical modeling of the material conversion, pyrolysis, and gas-phase combustion that replicate the experiments. Large-eddy simulations (LES) and eddy-dissipation concept (EDC) approach are incorporated in the gas phase along with multiple relevant reaction model methods in the solid phase. The numerical methods that use multi-step pyrolysis rate expressions are validated by thermogravimetric analysis (TGA) results. The pyrolyzed fuel components participate in gas-phase combustion using a turbulent combustion model. The multi-phase combustion capability was further assessed using two cases: a single particle reaction and a solid panel exposed to strong radiant heat. The panel fire test indicates that the model accurately reproduces panel temperature profile while a weaker oxidation is predicted.

Keywords: Carbon Fiber-Epoxy, Pyrolysis, Solid Combustion, Thermal Gravimetric Analysis (TGA)

1. Introduction

Composite materials are increasingly used in the manufacture of aircraft. In particular, carbon fiber-epoxy has gained popularity due to its light weight and strength. However, until recently, there was limited empirical data on fire scenarios that could ensue from a crash environment. Part of the empirical data are from calorimeter tests [1–3], rubble fire tests [4], and a radiative heat thermal test [5]. A more detailed review is found at Brown [6]. While these data are essential in understanding general combustion characteristics of the composite, only limited information that can be utilized for numerical modeling is presented.

Recently, several thermogravimetric analyzer (TGA) tests using carbon fiber-epoxy were published [7, 8], along with fitted pyrolysis mechanisms. The fitted reaction mechanism from [7] is used for simulating various reactive composite scenarios in this study.

---

[*] Sandia is a multiprogram laboratory operated by Sandia Corporation, a Lockheed Martin Company, for the United States Department of Energy under Contract No. DE-AC04-94AL85000.

2. Numerical Methods

Simulations are conducted using an unstructured control-volume finite-element code [9, 10], a component of Sandia National Laboratories SIERRA thermal-fluids code suite. The package has a capability of integrating different physics in multiple phases. SIERRA/Fuego, used for the current study, is a low-Mach flow solver suited for non-reacting and reacting flows. SIERRA/Fuego evolves temporally-filtered Navier-Stokes (TFNS) equations which are similar to large-eddy simulations (LES), but allow larger timesteps [9]. The subgrid-scale kinetic energy one-equation LES model is used to describe the subfilter process. Enthalpy and species mass fraction equations are also temporally-filtered.

Gas-phase combustion is closed with the eddy-dissipation concept (EDC) with fast chemistry [11]. An arbitrary hydrocarbon fuel is decomposed into CO and H_2 at the first step, while the intermediate species, CO and H_2, are further oxidized in the second step provided oxygen is still sufficient. This approach properly models CO, and potentially soot, in the fuel-rich case. Radiative heat transfer is handled by solving a radiation transport equation.

Material conversion of the solid-phase is modeled either on a panel located on the domain boundary or on a Lagrangian particle. Conversion into different material or different phase occurs following a set of reaction rates listed in Table 1. When the particle approach is used, a full two-way coupling with the gas-phase is included, using a point-particle assumption. Since the particle capability targets a TGA study (Sec. 3), which uses tiny samples, a uniform property assumption throughout the particle is used. The boundary panel approach mimics surface erosion of a test coupon as will be simulated in Sec. 4. Thickness, density, and other properties of the composite panel are given as initial conditions. Temperature and material composition profiles inside the panel are modeled by dividing the material into a given number of nodes. As decomposition takes place, the composition changes and mass transfer between gas and solid phases occurs. Surface regression is not considered in the panel boundary approach. Details of the model are available in Brown et al. [12].

Reaction rates in Table 1 are presented in unconventional form that involves different phases. When both solid and gas phases participate in a reaction as reactants, the pre-exponent factor is not a constant as it varies with gas density. If a reaction mechanism involves a 3rd reactant, the pre-exponent factor needs further modification reflecting the density of the 3rd reactant. This is a common issue when the mechanism is developed using mass fractions separately defined in each phase [7, 8].

For instance, the following are the methane and epoxy evolution equations. In the equations, $\omega_{\dot{E}DC}$ is gas-phase combustion source, and ρ_g and ρ_s are density in gas and solid phases, respectively.

$$\frac{\partial \rho_g Y_{CH_4}}{\partial t} + \nabla \cdot (\rho_g \mathbf{u} Y_{CH_4} + \rho_g D \nabla Y_{CH_4}) = \omega_{\dot{E}DC} + 0.5\dot{\omega}_1 + \dot{\omega}_2 \tag{1}$$

$$\frac{d\rho_s Y_{epoxy}}{dt} = -\dot{\omega}_1 - \dot{\omega}_2 \tag{2}$$

$\dot{\omega}_k$ is the reaction source from the kth mechanism in Table 1, which is in two following expressions depending on the mechanism. $Y_{r,s}$ and $Y_{r,g}$ are the mass fractions of the reactant solid material and the reactant gas phase species, respectively. A is the pre-exponent factor, E_a is the activation energy, R is the gas constant, and T is the temperature.

$$\dot{\omega_1} = \rho_s Y_{r,s} A e^{-E_a/RT} \tag{3}$$

$$\dot{\omega_{2-5}} = \rho_s Y_{r,s} \rho_g Y_{r,g} A e^{-E_a/RT} \tag{4}$$

Mechanism	A (1/s or m^3/kg-s)	E_a/R (K)	ΔH (kJ/kg)	Equation
Epoxy → 0.5CharA + 0.5CH_4	3.33E+15	27200	0	(3)
Epoxy + O_2 → CharB + CH_4	5.30E+15/ρ_g	27200	0	(4)
CharA + O_2 → Residue + CO	7.58E+02/ρ_g	10000	12730	(4)
CharB + O_2 → Residue + CO	7.58E+02/ρ_g	10000	12730	(4)
Carbon-Fiber + O_2 → Residue + CO_2	3.79E+15/ρ_g	38000	24770	(4)

Table 1: Pyrolysis and oxidation mechanism and rates for carbon-fiber epoxy [7].

Note that some reactions are exothermic. ΔH in Table 1 alters the temperature of the solid material. Density of the carbon fiber-epoxy is $1779 kg/m^3$, and the emissivity is assumed as 0.85.

3. Single Particle Evolution

TGA tests were used to calibrate the pyrolysis and oxidation mechanism of carbon fiber-epoxy [7, 8]. The test was replicated in a full 3D fluid calculation to understand interactions of the sample with surrounding flows. A non-movable composite particle sample with a diameter of $50\mu m$ was placed in a 4cm×2cm×2cm domain (Fig. 1). The mesh size was 2mm. The air stream velocity was fixed at 2cm/s and the temperature slowly increased until the sample was depleted. Gas density is at 1 atm and 700^oC, and was used to correct the pre-exponent factors in Table 1. Heat release from the oxidation was neglected.

Figure 2 shows the predicted mass change of the material being consumed or generated during pyrolysis. The profile closely matches the reference ([7]) since the same mechanism is used. Before reaching 450^oC, epoxy pyrolysis creates char A and epoxy oxidation generates char B (only char A is plotted in Fig. 2). The carbon-fiber and the chars oxidize at a substantially higher temperature. Pyrolysis response to different heating rates is correctly predicted as plotted in Fig. 2. In particular, both pyrolysis and oxidation are delayed as the heating rate increases. Phase conversion rate is higher in the oxidation process than the initial epoxy pyrolysis.

4. Composite Panel

SIERRA/Fuego was tested on a heated composite panel scenario where the material decomposes and burns when subjected to fire-like radiative heat fluxes. The domain shown in Fig. 3 is a simplified representation of an experiment performed by Hubbard et al. [5]. A composite panel with a size of 0.102m×0.076m was located in the middle of the bottom surface. The thickness of the panel was 3.2mm. Radiative heat flux originated from a hot 0.184m×0.184m surface on the top. The distance between the heat source and the composite panel was 0.14m. An adiabatic condition was assumed for all the other walls including the back side of the panel. The mesh size was 12.5mm and the total number of elements was approximately 11,000. This effort demonstrates coupling capabilities between flow fields, heat transfer, pyrolysis, and radiation. Temperature variation in the panel depth direction was ignored and the combustion model was turned off.

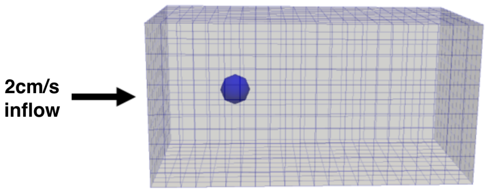

Figure 1: The mesh for the single particle TGA calculation. Particle size is exaggerated.

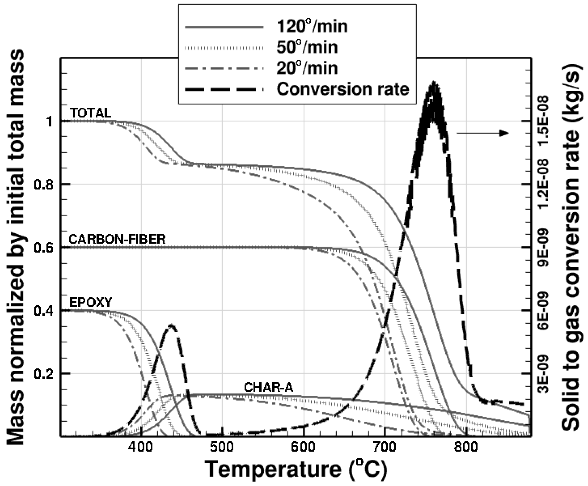

Figure 2: Predicted mass changes of the single particle evolution for different heating rates. Conversion rate is from the fastest heating rate case.

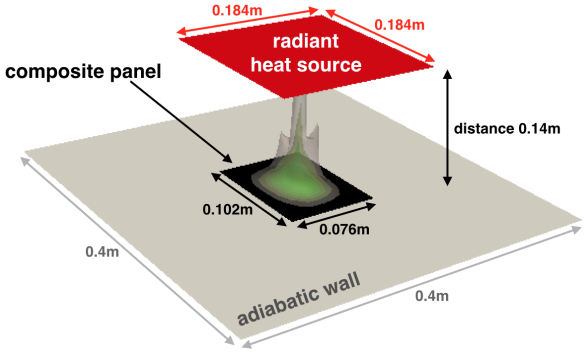

Figure 3: The computational domain for the composite panel case. Omitted here is the wall at the top surface around the heat source. Isocontours of a decomposed gas from the panel is shown in the middle.

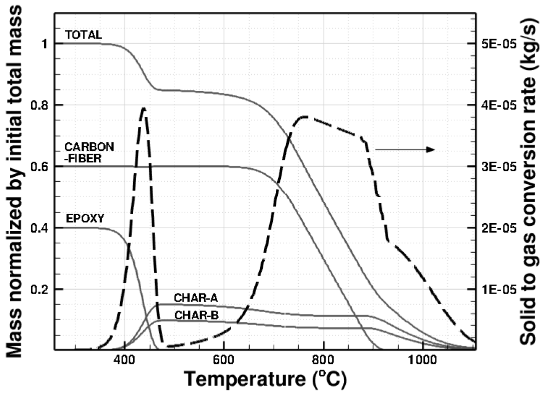

Figure 4: Mass changes of the composite panel under a slow heating rate, 120^{o}C/min, and a faster flow, 2m/s.

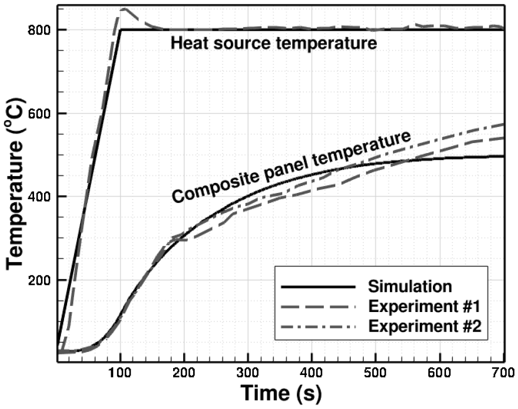

Figure 5: Temperature profiles of the controlled heat source and the heated panel.

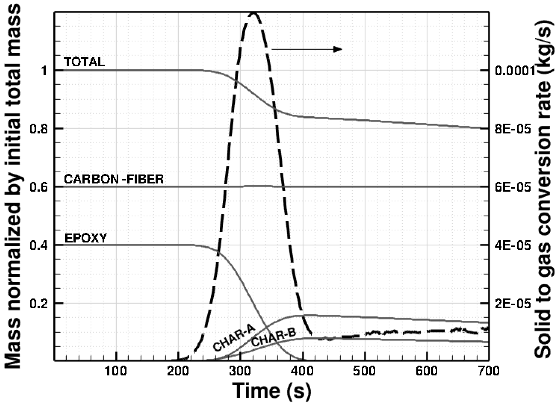

Figure 6: Panel mass changes and conversion rate with a radiant heat source and quiescent flow.

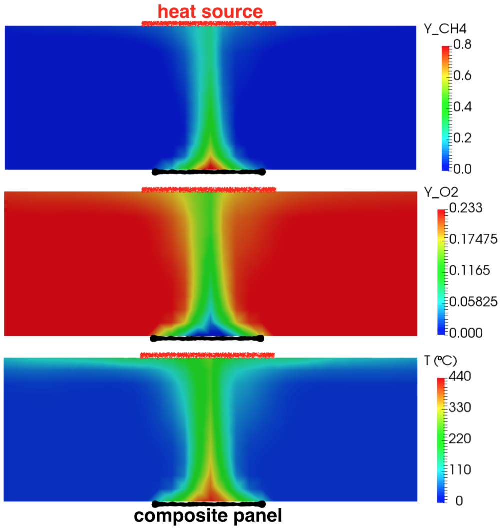

Figure 7: Contours of the center plane at 310s.

For validation purposes, the panel was exposed to a slow heating rate similar to the TGA condition. A thinner panel (0.32mm) was used for this calculation and a rather fast 2m/s horizontal flow was imposed. The result is plotted in Fig. 4. Compared to the single particle calculation (Fig. 2), epoxy pyrolysis and oxidation initiation occur at similar temperature ranges. However, the composite panel oxidizes much slower than the composite particle. The delay is attributed to oxygen blockage above the panel despite the flow. Due to the slower oxidation, peak conversion rates between epoxy pyrolysis and oxidation are comparable (Fig. 4).

The temperature of the heat source (as shown in Fig. 5) follows close to the experimental condition. The simulation started from zero flow velocity. The conversion mass rate and temperature profile at the back side of the panel are also plotted in Figs. 5 and 6. As radiant heat flux increases, the panel begins to pyrolyze until all of the epoxy is consumed (Fig. 6). Oxidation, however, is very slow, resulting in minimal conversion rate once epoxy pyrolysis is over. As shown in Fig. 7, lack of oxygen near the panel significantly delays oxidation process. Moreover, the panel does not reach high enough temperature for an active oxidation.

The back side temperature profile compares well to two experiment data that were measured under the same condition [5] (Fig. 5). It is reported that visible gasification occurred between 165s and 660s in one experiment (marked as #1 in Fig. 5), and between 100s and 520s in the other (#2 in Fig. 5). Note that lack of uniformity of the composite resulted in different results, such as #1 and #2 profiles in Fig. 5, even with the identical experimental condition. The simulation shows higher mass flow rate (10% of peak conversion rate, or 1.2E-5kg/s) between 240s and 400s, which begins later and finishes earlier than the experiment (Fig. 6). The conversion that continues after 400s appears weaker, although it is not clear whether the small conversion rate such as 1E-5kg/s would be visible in the experiments. Reported panel shape changes (such as swelling) and their effects were ignored in the simulation.

The simulation predicts ignition as soon as the gas-phase reaction model is turned on. However, burning was not observed in the experiment. The discrepancy is attributed to excessive amount of methane produced in the epoxy pyrolysis, along with poor ignition predictability of the turbulent combustion model. Note that the pyrolysis and oxidation mechanisms focus on the solid-phase response while generated gas-phase species were not measured. Future work should focus on determining detailed pyrolysis products appropriate to model the system. The first step will be the introduction of a model for generation and cracking of tar.

References

[1] B. Kandola, F. Sarker, P. Luangtriratana, and P. Myler, Thermal Protection of Carbon Fiber-Reinforced Composites by Ceramic Particles, Coatings 6 (2016).

[2] D. Q. Dao, T. Rogaume, J. Luche, F. Richard, L. B. Valencia, and S. Ruban, Thermal degradation of epoxy resin/carbon fiber composites: Influence of carbon fiber fraction on the fire reaction properties and on the gaseous species release, Fire and Materials 40 (2016) 27–47.

[3] G. Kalogiannakis, D. Van Hemelrijck, and G. Van Assche, Measurements of thermal properties of carbon/epoxy and glass/epoxy using modulated temperature differential scanning calorimetry, Journal of Composite Materials 38 (2004) 163–175.

[4] A. L. Brown and B. Servantes, Composite Rubble Fire Test Results, Report No. SAND2017-(in preparation), Sandia National Laboratories, Albuquerque, NM, USA, 2017.

[5] J. A. Hubbard, A. L. Brown, A. B. Dodd, S. Gomez-Vasquez, and C. J. Ramirez, Carbon fiber composite characterization in adverse thermal environments, Report No. SAND2011-2833, Sandia National Laboratories, Albuquerque, NM, USA, 2011.

[6] A. Brown, The decomposition behavior of thermoset carbon fiber composites in the fire environment, The 8th US National Combustion Meeting (2013).

[7] A. B. Dodd, B. Shelden, and K. L. Erickson, Numerical Simulation of Decomposition and Combustion of an Epoxy-Carbon-Fiber Composite, 13th International Conference and Exhibition on Fire Science and Engineering (2013).

[8] J. G. Quintiere, R. N. Walters, and S. Crowley, Flammability Properties of Aircraft Carbon-Fiber Structural Composite, Report No. DOT/FAA/AR-07/57, Air Traffic Organization Operations Planning Office of Aviation Research and Development Washington, DC, USA, 2007.

[9] S. R. Tieszen, S. P. Domino, and A. R. Black, Validation of a Simple Turbulence Model Suitable for Closure of Temporally-Filtered Navier-Stokes Equations Using a Helium Plume, Report No. SAND2005-3210, Sandia National Laboratories, Albuquerque, NM, USA, 2005.

[10] A. Luketa, V. Romero, S. Domino, D. Glaze, M. Sherman, and V. Figueroa, Validation and uncertainty quantification of Fuego simulations of calorimeter heating in a wind-driven hydrocarbon pool fire, Report No. SAND2009-7605, Sandia National Laboratories, Albuquerque, NM, USA, 2009.

[11] B. F. Magnussen, On the Structure of Turbulence and a Generalised Eddy Dissipation Concept for Chemical Reactions in Turbulent Flow, 9th AIAA Aerospace Science Meeting (1981).

[12] A. Brown, D. Glaze, and F. Pierce, Sensitivity Analysis and Verification of a 1-D Surface Solid Combustion Model for a Fire CFD Boundary Condition, 11th AIAA/ASME Joint Thermophysics and Heat Transfer Conference (2014).